Determining the spin of supersymmetric particles at the LHC using lepton charge asymmetry.

A.J. Barr

Cavendish Laboratory, University of Cambridge, Madingley Road, Cambridge, CB3 0HE, UK

Abstract

If signals suggesting supersymmetry (SUSY) are discovered at the LHC then it will be vital to measure the spins of the new particles to demonstrate that they are indeed the predicted super-partners. A method is discussed by which the spins of some of the SUSY particles can be determined. Angular distributions in sparticle decays lead to charge asymmetry in lepton-jet invariant mass distributions. The size of the asymmetry is proportional to the primary production asymmetry between squarks and anti-squarks. Monte Carlo simulations are performed for a particular mSUGRA model point at the LHC. The resultant asymmetry distributions are consistent with a spin-0 slepton and a spin-$\frac{1}{2}$ $\tilde{\chi}_2^0$, but are not consistent with both particles being scalars.

Key words: Hadronic Colliders, Supersymmetry, Spin, LHC
Cavendish HEP-2004-14

1 Spin correlations and charge asymmetry

A recent publication [1] describes the method by which spin correlations were added to the `HERWIG` [2,3] Monte Carlo event generator. It includes an example of part of a supersymmetric decay chain,

$$\tilde{q}_L \to \tilde{\chi}_2^0 q_L \to \tilde{l}_R^{\pm} l^{\mp} q_L \tag{1}$$

in which spin correlations can play a significant role in the kinematics of the emitted particles. When the decay of the slepton is also considered, (fig. 1),

Email address: `alan.barr@cern.ch` (A.J. Barr).

the final state consists of two opposite-signed leptons of the same family, a quark jet, and missing energy from the undetected $\tilde{\chi}_1^0$.

In this Letter I examine the observability of spin effects in this decay chain at the LHC. I first consider the distribution of invariant mass of the quark or anti-quark jet from the squark decay, and the lepton or anti-lepton from the $\tilde{\chi}_2^0$ decay. Using the terminology of [4], this lepton is referred to as the 'near' lepton, as opposed to the lepton from the slepton decay, which is called the 'far' lepton. Initially I investigate the parton-level distributions which one would obtain if the sign of the squark and the identity of the lepton were known. In section 4 the experimentally observable distributions are introduced. These have added complications due to the difficulty in (a) distinguishing which lepton came from which decay, and (b) measuring the charge of the (s)quark.

In the approximation in which the quark and lepton are massless, and the SUSY particles are on-mass-shell, then the $l^{\rm near}q$ invariant mass has a simple and direct interpretation in terms of the angle, θ^*, between the quark and lepton in the $\tilde{\chi}_2^0$ rest frame,

$$\left(m_{lq}^{\rm near}\right)^2 = 2|\mathbf{p}_l||\mathbf{p}_q|(1-\cos\theta^*) = \left(m_{lq}^{\rm near}\right)^2_{\rm max}\sin^2(\theta^*/2) \tag{2}$$

where $\mathbf{p}_l$ and $\mathbf{p}_q$ are the 3-momenta of the near lepton and the quark respectively in the $\tilde{\chi}_2^0$ rest frame, and the kinematic maximum of $m_{lq}^{\rm near}$ is given by

$$\left(m_{lq}^{\rm near}\right)^2_{\rm max} = (m^2_{\tilde{q}_L} - m^2_{\tilde{\chi}_2^0})(m^2_{\tilde{\chi}_2^0} - m^2_{\tilde{l}_R})/m^2_{\tilde{\chi}_2^0}\ . \tag{3}$$

As one would expect, for events in which $m_{lq}^{\rm near}$ is at its maximum value $\sin^2(\theta^*/2) = 1$, *i.e.* $\theta^* = \pi$, and the near lepton and the quark are back-to-back in the rest frame of the $\tilde{\chi}_2^0$.

If the spin correlations were ignored, and particles were allowed to decay according to phase-space, then the probability density function would be

$$\frac{dP_{\rm PS}}{d\hat{m}} = 2\sin(\theta^*/2) = 2\hat{m} \tag{4}$$

where the rescaled invariant mass variable, $\hat{m}$, is defined by

$$\hat{m} \equiv m_{lq}^{\rm near}/\left(m_{lq}^{\rm near}\right)_{\rm max} = \sin(\theta^*/2)\ . \tag{5}$$

Taking spin correlations into account, there are extra spin projection factors in the amplitude of $\sin(\theta^*/2)$ or $\cos(\theta^*/2)$ depending on the helicities of the

(anti)lepton and (anti)quark, so that for l^+q or $l^-\bar{q}$

$$\frac{dP_1}{d\hat{m}} = 4\sin^3(\theta^*/2) = 4\hat{m}^3 \tag{6}$$

while for l^-q or $l^+\bar{q}$

$$\frac{dP_2}{d\hat{m}} = 4\sin(\theta^*/2)\cos^2(\theta^*/2) = 4\hat{m}(1-\hat{m}^2)\ . \tag{7}$$

The functional form of these distributions is shown in fig. 2.

2 Parton level

I take as an example model the mSUGRA point with $m_0 = 100$ GeV, $m_{\frac{1}{2}} = 300$ GeV, $A_0 = 300$ GeV, $\tan\beta = 2.1$ and $\mu > 0$. For this point the decay chain (fig. 1) has already been well investigated in the context of sparticle mass measurements [4,5]. The point was originally motivated by cosmological $\tilde{\chi}_1^0$ relic density considerations, but it has subsequently been excluded by the LEP light Higgs limit [6]. This has no bearing on the analysis presented in this Letter, since the point is used only to illustrate the method.

The SUSY mass spectrum and decay branching ratios were calculated with `ISAJET-7.64`. Some of the important sparticle masses are shown in table 1. These values differ from those of [4, 5] because a more recent version of the `ISAJET` program has been used with updated renormalization group evolution. One significant point to mention in respect to this analysis is that the $\tilde{\chi}_2^0$ is largely Wino, so the branching ratios $\tilde{q}_R \to \tilde{\chi}_2^0 q$ are highly suppressed compared to the equivalent decays for the left-handed squarks.

To examine the parton-level distributions, a small sample of inclusive SUSY events (≈ 2.5 fb^{-1}) was generated using the `HERWIG-6.505` Monte Carlo event generator, with the leading-order parton distribution functions of `MRST` [7] (average of central and higher gluon). There is an obvious difference between the $l^{\rm near}q$ distributions for leptons and anti-leptons (fig. 3a). The differences between these shapes and those in the idealized distributions (fig. 2) are largely due to sparticles being off their mass shells and contributions from the various different-mass squarks.

$\tilde{g}$	$\tilde{\chi}_1^0$	$\tilde{\chi}_2^0$	$\tilde{u}_L$	$\tilde{d}_L$	$\tilde{e}_R$	$\tilde{e}_L$
717	116	213	631	634	153	229

Table 1
Masses of selected particles (in GeV) for the model point investigated.

The distinctive charge asymmetry is caused by spin correlations carried by the spin-$\frac{1}{2}$ $\tilde{\chi}_2^0$, so if one could measure the m_{lq}^{near} invariant mass distribution in the decay chain (1) it would be easy to show that the $\tilde{\chi}_2^0$ is spin-$\frac{1}{2}$.

However there are experimental difficulties in making such a measurement. As was noted in [1], in the decay of an anti-squark the asymmetry in the lepton charge distributions is in the opposite sense to that from squark decays (see fig. 3b). As it is experimentally unlikely that one could distinguish between a quark and an anti-quark jet at the LHC, only the sum of the lq and $l\bar{q}$ distributions can be considered to be observable. Thus, if equal numbers of squarks and anti-squarks were produced, the $l^{\text{near}}q$ distribution would be indistinguishable from the phase-space distribution, and no spin information could be obtained. However the fact that the LHC will be a proton-proton collider means that the production of squarks will be enhanced compared to anti-squarks, which can then lead to a significant spin-generated lepton charge asymmetry.

3 $\tilde{q} - \bar{\tilde{q}}$ production asymmetry

In a pp collider, the production processes

$$qg \to \tilde{q}\tilde{g} \quad \text{and} \quad \bar{q}g \to \bar{\tilde{q}}\tilde{g} \tag{8}$$

will produce more squarks than anti-squarks. This is because the quark parton distribution function (PDF) is larger than that of the anti-quark due to the presence of the valence quarks.

For a significant $\tilde{q} - \bar{\tilde{q}}$ asymmetry, the processes (8) must provide a significant contribution to the (anti)squark production. That is to say that they must not be much smaller than competing charge-symmetric processes such as

$$q\bar{q} \to \tilde{q}\bar{\tilde{q}} \quad , \quad gg \to \tilde{q}\bar{\tilde{q}} \tag{9}$$

or gluino pair production followed by decay to (anti)squarks. One must also check that the processes (8) sample the parton distribution functions in a region of x and μ_F^2 where valence quark PDFs are significant.

It is safe to assume that by the time SUSY spin measurements are being made at the LHC, the PDFs will be well measured from other measurements, for example from electroweak boson production. One would expect that the production asymmetry, which is the result of the well measured valence quark distribution, would be insensitive to any remaining uncertainty in the PDFs.

The Bjorken $x_{1,2}$ parameters, giving the fraction of the proton momenta carried by the initial state partons satisfy

$$x_1 x_2 = M^2/s \ , \tag{10}$$

where s is the usual Mandelstam variable. For the LHC, $\sqrt{s} = 14$ TeV, and for the test point the invariant mass, M, for squark pair production is about 1.3 TeV, so the x_i can be expected to be of the order of 0.1. This is confirmed from the values of x sampled by the Monte Carlo (fig. 4b).

In terms of producing a $\tilde{q} - \bar{\tilde{q}}$ asymmetry, it is advantageous that at $x \approx 0.1$ and $\mu_F^2 \sim 1$ TeV^2 the valence quark parton distribution functions are large (fig. 4a). The over-production of squarks relative to anti-squarks for the test point can be observed by comparing the normalisation of the lq and $l\bar{q}$ plots in fig. 3, where it can be seen that approximately twice as many squarks are produced as anti-squarks for this point.

4 Experimental observables

Although the $l^{\text{near}}q$ invariant mass would provide the theoretically cleanest spin signature, with the experimental data it will not be possible to distinguish the near lepton (from the $\tilde{\chi}_2^0$ decay) from the far lepton (from the $\tilde{l}_R^{\pm}$ decay) on an event-by-event basis. Since all of these signal events will contain two leptons of the same family but of different sign, what one *can* do experimentally is to look for asymmetries in the l^+q and l^-q distributions, each of which will contain contributions from both the near and the far lepton.

The asymmetry in the $l^{\text{near}}q$ invariant mass was discussed in section 2. One might naively assume that the invariant mass distribution of the far (anti)-lepton with the (anti)quark would be free from spin-correlation effects, since this lepton originates from the decay of a scalar particle, the $\tilde{l}_R^{\pm}$, which should wash out any spin effects. However the slepton itself has been produced in the decay of the $\tilde{\chi}_2^0$, and so has a boost relative to the quark jet which depends on its charge. To be explicit about the sense of the difference, recall that the near positive lepton favours being back-to-back with a q jet. This decreases the boost of the negative slepton relative to the q jet, and means that on average the invariant mass of the quark with a negative far lepton will be smaller than with a positive lepton. The $l^{\text{far}}q$ invariant mass distributions are shown in fig. 5a while the equivalent distributions from anti-squark decay, $m_{l\bar{q}}^{\text{far}}$, are plotted in fig. 5b.

The l^+q and l^-q distributions contain contributions from both near and far leptons, and from squark and anti-squark decays. The spin information carried

by the $\tilde{\chi}_2^0$ causes an obvious difference in shape between these experimentally-accessible distributions (fig. 6a). The charge asymmetry in the differential cross-sections is defined here as

$$A^{+-} \equiv \frac{s^+ - s^-}{s^+ + s^-}, \quad \text{where} \quad s^{\pm} = \frac{d\sigma}{d(m_{l^{\pm}q})} \ . \tag{11}$$

This asymmetry, plotted as a function of m_{lq} in fig. 6b, is clearly not consistent with zero. This demonstrates that at parton level the asymmetry survives contamination from anti-squark production, and the experimental lack of knowledge of near vs. far lepton.

To check that this asymmetry is robust, a 500 fb^{-1} sample of inclusive SUSY events was generated with `HERWIG` at the same mSUGRA point. The events were then passed through the `ATLFAST-2.50` [8] detector simulation.

The cuts applied are taken directly from a previous analysis [4] in which it was emphasised that this selection had not been tuned to the particular mSUGRA point under investigation, and so could claim a degree of model-independence.

In brief, the event selection requires:

- exactly 2 electrons or muons of the same family with opposite charge, both having $p_T \geq 10$ GeV.
- four or more jets with $p_T^{j_1} \geq 100$ GeV and $p_T^{j_k} \geq 50$ GeV for $k \in \{2,3,4\}$, where $p_T^{j_i}$ is the transverse momentum of the ith jet ordered in p_T such that $p_T^{j_1} > p_T^{j_2} > p_T^{j_3} > p_T^{j_4}$.
- missing transverse momentum, $\not{p}_T \geq \max(100\,\text{GeV}, 0.2\,M_{\text{effective}})$ and $M_{\text{effective}} \geq 400$ GeV, where $M_{\text{effective}} = \not{p}_T + \Sigma_{i=1}^{4} p_T^{j_i}$
- dilepton invariant mass, $m_{ll} \leq m_{ll}^{\max} + 1$ GeV
- dilepton plus jet invariant mass, $m_{llq} \leq m_{llq}^{\max}$ where $m_{llq} = \min(m_{llj_1}, m_{llj_2})$.

A more detailed discussion of this selection, including the definition of the kinematic limits $m_{ll}^{\max}$ and $m_{llq}^{\max}$ is offered in [4]. After applying these cuts the remaining Standard Model background has been shown to be much smaller than the SUSY background [5], and so has not been simulated here.

For real data, one would expect that charge-blind $m_{l^{\pm}q}$ and other invariant mass distributions would be investigated first. One would use these to extract information on the mass of the various sparticles. Using this information, the selection parameters could be tuned before making any attempt to measure the lepton charge asymmetry, however no such tuning has been attempted for this Letter.

While the shapes of the $m_{l^{\pm}q}$ distributions (fig. 7a) are modified by detector simulation and event selection, the cuts are charge-blind, and so the detector-

level asymmetry function (fig. 7b) retains the same approximate shape as at parton level. To help visual comparison the parton-level asymmetry has been scaled down by a factor of 0.6. A decrease in the observed asymmetry can be expected due to pollution from the SUSY background. A more sophisticated analysis could estimate this background as a function of m_{lq} using a same-sign dilepton event selection. Some smearing is apparent, but the fact that the asymmetry is negative at low m_{lq}^{near} and positive at high m_{lq}^{near} is very clear. The shape of the asymmetry function therefore strongly favours a spin-$\frac{1}{2}$ $\tilde{\chi}_2^0$.

A nice contrast can be seen by making a cross-check in which the spin correlations have been switched off in the Monte Carlo so that all particles decay according to pure phase-space. This produces no significant asymmetry (fig. 7b) and reflects in some sense the experimental expectation for a 'scalar $\tilde{\chi}_2^0$'.

Figure 7b was made with a high-statistics (500 fb^{-1}) sample so that the shape of the distribution could be clearly seen. However such a large sample is not necessarily required to determine that the spin correlations exist. The integrated luminosity required to make the measurement will be different for each SUSY point, depending on the sparticle spectrum. However for the particular mSUGRA point investigated, the spin-generated charge asymmetry can be seen to be inconsistent with zero with 150 fb^{-1} of integrated luminosity (fig. 7c).

It is worth adding that further spin information is available from the dilepton invariant mass distribution. This also has a kinematic limit, this time at

$$(m_{l^+l^-})^2_{\text{max}} = (m^2_{\tilde{\chi}_2^0} - m^2_{\tilde{l}_R})(m^2_{\tilde{l}_R} - m^2_{\tilde{\chi}_1^0})/m^2_{\tilde{l}_R} \ . \tag{12}$$

Since one lepton of either sign is produced, and both are right-handed, one might expect that the angular distribution would show strong spin effects. However the scalar slepton removes all spin correlations between the leptons, and so the $m_{l^+l^-}$ distribution (fig. 7d) is in very good agreement with the triangular prediction of phase-space (fig. 2). This agreement would be hard to explain except as a result of a heavy scalar particle carrying lepton number, and so would increase confidence in the supersymmetric nature of the particles participating in the decay chain.

5 Conclusions

The method presented shows that it is possible to determine the spins of some of the SUSY partners of Standard Model particles at the LHC. The charge asymmetry lends good supporting evidence to the hypothesis that one is observing supersymmetry and to the identity of the sparticles participating in the

decay chain. For the point examined, the shape of the asymmetry distribution could be observed with an integrated luminosity of 150 fb^{-1}.

It should be noted that the method presented here requires a particular decay chain (fig. 1) to occur at a reasonably high rate, and an initial asymmetry in the squark vs. anti-squark production cross-sections. However, it could be employed to disentangle supersymmetry from other phenomenologically interesting models, such as universal extra dimensions with Kaluza-Klein parity [9].

Acknowledgments

I would like to thank my colleagues in the Cambridge SUSY working group for helpful discussions, particularly Bryan Webber and Chris Lester. I am also pleased to thank Robert Thorne, and the members of the Oxford ATLAS particle physics group, especially Claire Gwenlan, for discussions relating to parton distribution functions. I have made use of the physics analysis framework and tools which are the result of ATLAS collaboration-wide efforts. This work was funded by PPARC.

References

[1] P. Richardson, JHEP 11 (2001) 029.

[2] G. Corcella, et al., JHEP 01 (2001) 010.

[3] S. Moretti, K. Odagiri, P. Richardson, M. H. Seymour, B. R. Webber, JHEP 04 (2002) 028.

[4] C. G. Lester, Ph.D. thesis, CERN-THESIS-2004-003 (2002).

[5] ATLAS Detector and Physics Peformance TDR, CERN, 1999.

[6] R. Barate, et al., Phys. Lett. B565 (2003) 61–75.

[7] A. D. Martin, R. G. Roberts, W. J. Stirling, R. S. Thorne, Eur. Phys. J. C4 (1998) 463–496.

[8] E. Richter-Was, D. Froidevaux, L. Poggioli, ATLAS note ATL-PHYS-98-131.

[9] H.-C. Cheng, K. T. Matchev, M. Schmaltz, Phys. Rev. D66 (2002) 056006.

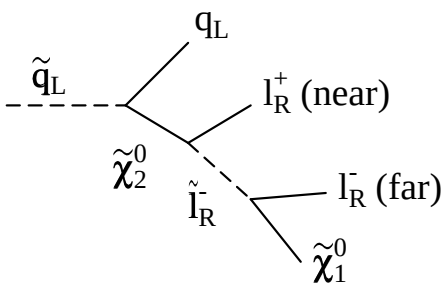

Fig. 1. The decay chain under investigation. The lepton from the $\tilde{\chi}_2^0$ decay is labeled the 'near' lepton, regardless of its charge. Also considered are the diagrams after charge conjugation of the slepton and leptons; or of the squark and quark; or of the entire diagram.

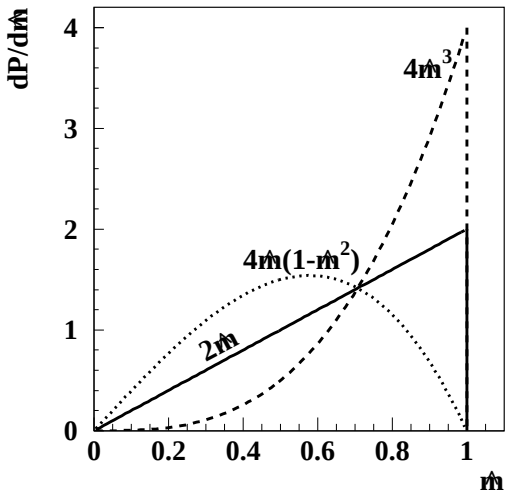

Fig. 2. Idealised shapes of the $l^{\text{near}}q$ invariant mass distributions in terms of the re-scaled invariant mass variable $\hat{m}$ defined in eq. 5. The solid line shows $\frac{dP_{\text{PS}}}{d\hat{m}}$ (eq. 4), the dashed line $\frac{dP_1}{d\hat{m}}$ (eq. 6), and the dotted line $\frac{dP_2}{d\hat{m}}$ (eq. 7).

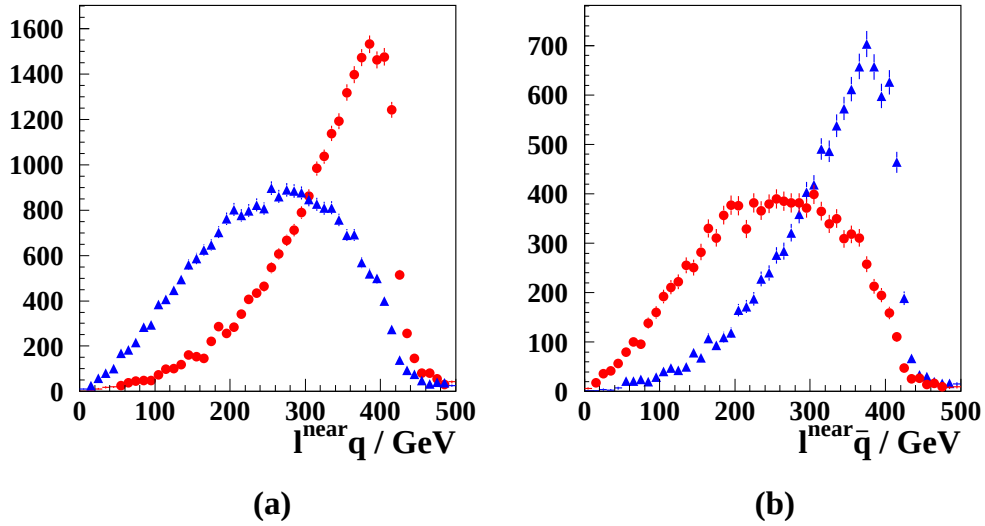

Fig. 3. Invariant mass distributions of **(a)** $l^{\rm near}q$ and **(b)** $l^{\rm near}\bar{q}$, at the parton level. The triangles are for a negatively charged near lepton, while the circles are for a positively charged near lepton. For the test point the on-shell kinematic maximum is 413.4 GeV. Note that these distributions cannot be measured directly by the experiment.

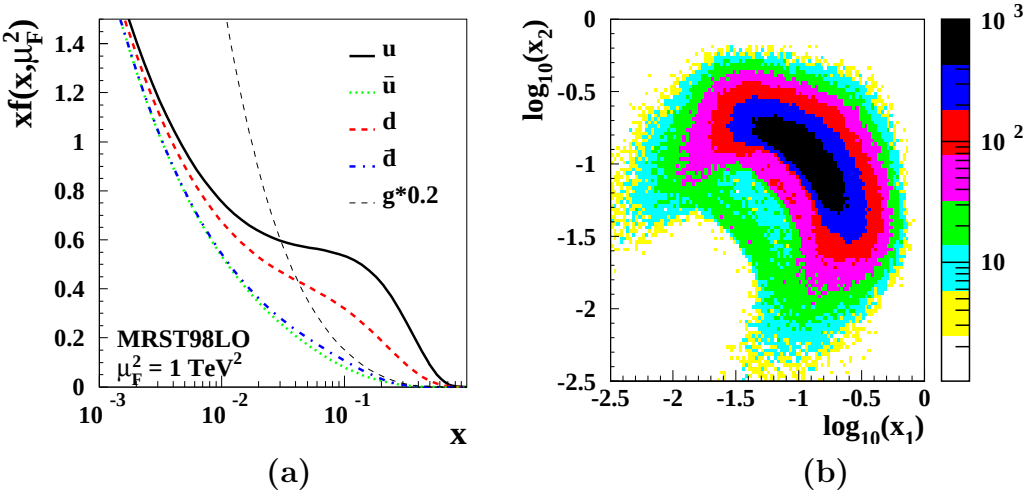

Fig. 4. **(a)** The parton distribution functions used in this Letter plotted at factorization scale $\mu_F^2 = 1$ TeV^2 [7]. **(b)** 2-dimensional histogram of the values of x_1 and x_2 sampled by the Monte Carlo in sparticle pair production at the mSUGRA point investigated.

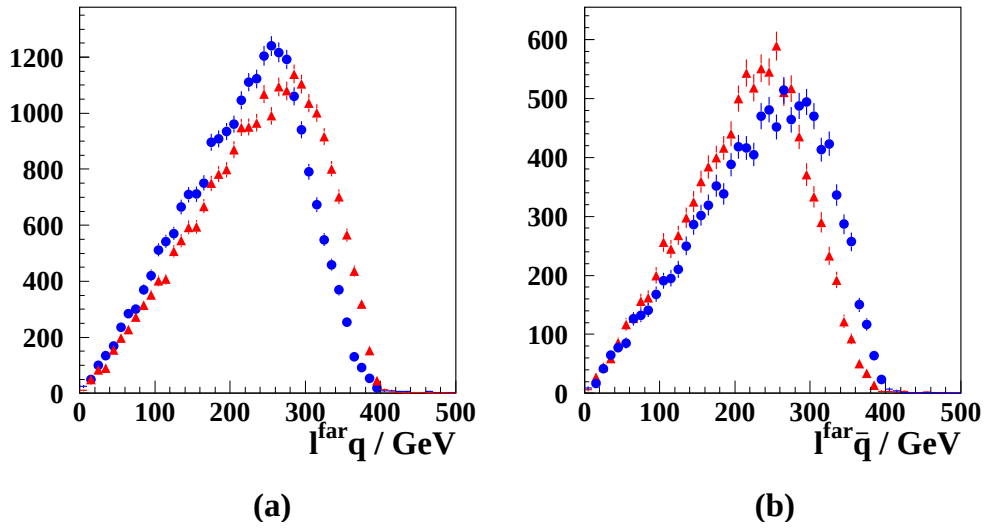

Fig. 5. Invariant mass distributions of **(a)** $l^{\rm far}q$ and **(b)** $l^{\rm far}\bar{q}$, at the parton level. The circles indicate the distribution for the negatively charged far lepton, while the triangles are for the positively charged far lepton. Note that these distributions, like fig. 3, cannot be directly measured by the experiment. The explanation for the charge asymmetry is given in the text.

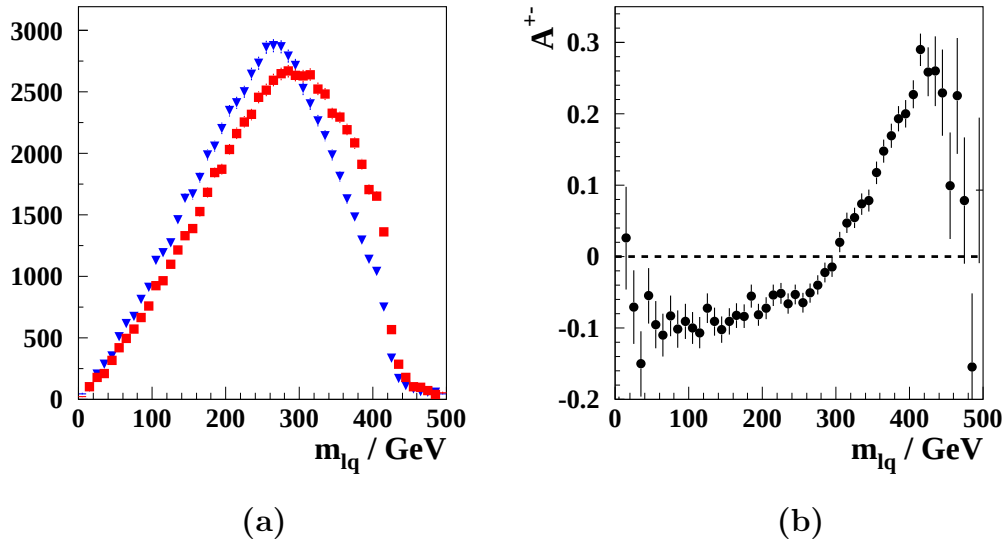

Fig. 6. **(a)** The l^+q (squares) and l^-q (triangles) invariant mass distributions, and **(b)** the charge asymmetry A^{+-} (eq. 11) at the parton level. These distributions have folded-in the indistinguishability of the near and far leptons, and quark vs. anti-quark jets.

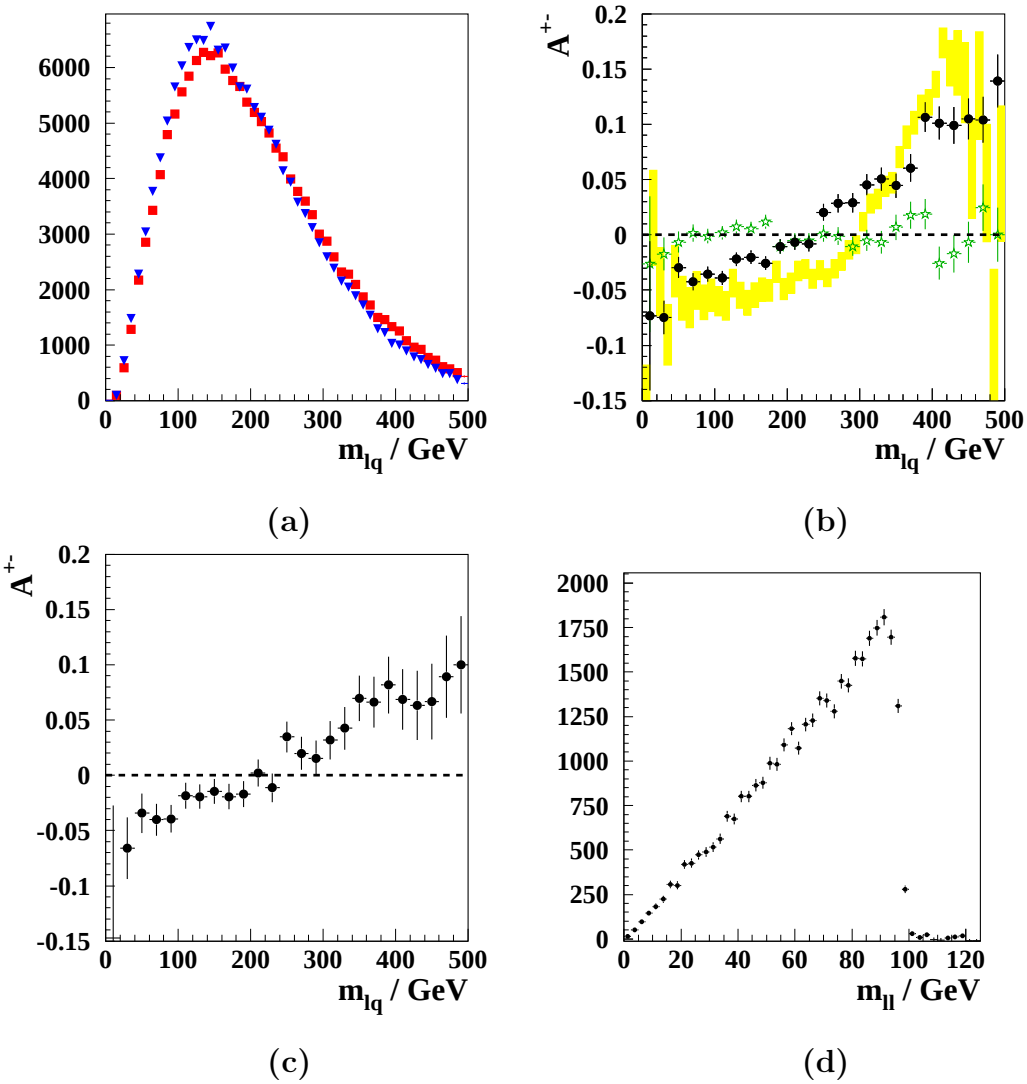

Fig. 7. **(a)** The l^+q (squares) and l^-q (triangles) invariant mass distributions after detector simulation and event selection. **(b)** The solid circles show the lepton charge asymmetry A^{+-} as a function of m_{lq}, again after detector simulation. The shaded rectangles are the parton-level result scaled down by a factor of 0.6. The stars show a cross-check – the equivalent detector-level asymmetry with spin correlations suppressed. For both of the upper two plots $\int Ldt = 500$ fb^{-1}. **(c)** The detector-level charge asymmetry, A^{+-}, with spin correlations, using a 150 fb^{-1} subset of the data. **(d)** The opposite-sign, same-family dilepton invariant mass distribution after opposite-sign, different-family subtraction.

Fig. 8.